Estimation of Hydraulic Conditions of Tsunami from Deposits: Inverse Model using Deep-Learning Neural Network

Rimali Mitra[1], Hajime Naruse[1], and Tomoya Abe[2]

[1]Division of Earth and Planetary Sciences, Graduate School of Science, Kyoto University, Kitashirakawa Oiwakecho, Kyoto, Japan.

[2]Research Institute of Geology and Geoinformation, Geological Survey of Japan, National Institute of Advanced Industrial Science and Technology (AIST), Tsukuba, Japan.

Key Points:

- Inverse modeling of paleo-tsunami deposits was performed using deep learning neural networks.
- 2011 Tohoku-Oki tsunami's flow velocity, maximum depth and inundation length, and sediment concentration were evaluated with inverse model.
- Comparison of observations and uncertainty analysis implied that the reconstructed flow conditions were accurate and reasonably precise.

Corresponding author: Rimali Mitra, mitra.rimali.37z@st.kyoto-u.ac.jp

Abstract

Tsunami deposits provide information for estimating the magnitude and flow conditions of paleo-tsunamis, and the inverse model has potential for predicting hydraulic conditions of tsunamis from their deposits. Majority of the previously proposed models are based on oversimplified assumptions and share limitations in applicability to original tsunami hydrodynamics in transportation and deposition settings. We present a new inverse model that serves as a modified version of the previously proposed model FITTNUSS, which incorporates nonuniform and unsteady transport of suspended sediment and turbulent mixing. The present model uses the deep neural network (DNN) for the inversion method. In this method, forward model calculation was repeated at random initial flow conditions to produce artificial training data sets that represent depositional characteristics such as thickness and grain size distribution. Subsequently, the DNN was trained for establishing the general inverse model based on artificial data sets derived from the forward model. Tests conducted using independent artificial data sets indicated that the established DNN can reconstruct the original flow conditions from the characteristics of the deposits. Finally, the model was applied to a data set of 2011 Tohoku-Oki tsunami deposits. Jackknife resampling was applied for estimating the precision of the result. The estimated results of the flow velocity and maximum flow depth were approximately 5.4 $\pm$0.140 m/s and 4.11 $\pm$0.152 m, respectively after the uncertainty analysis. The DNN showed promising results for reconstruction of the event from natural data set, which would help in estimating the hydraulic conditions of paleo-tsunamis based on realistic settings of tsunami deposits.

Plain Language Summary

This study presents an inverse model comprising the use of an artificial intelligence technique to estimate the hydraulic conditions of paleo-tsunamis based on realistic settings of tsunami deposits.

1 Introduction

Tsunami is one of the most disastrous natural hazards that occur in coastal zones. It is a threat to the overall socio-economic infrastructure of coastal-based cities (Lin et al., 2012). Tsunami hazard assessment is necessary for any fast-growing coastal city. The 2004 Indian Ocean tsunami and 2011 Tohoku-Oki tsunami caused devastating damage

to many Asian countries and Japan, but such situations are worsened when countries lack tsunami-related preparedness for disasters that cause human causalities and extensive building damage (Imamura et al., 2019). Ghobarah et al. (2006) reported that the debris carried by the 2004 Indian Ocean tsunami could cause major building damage. The 2004 Indian Ocean tsunami caused extensive structural and non-structural destruction of reinforced concrete buildings (Saatcioglu et al., 2005).

To mitigate tsunami disasters, a method of inverse modeling of tsunamis based on their geologic records has been developed. Tsunami deposits are defined as layers of sediment formed by hydrodynamic activities of tsunami, and research on tsunami deposits started since early 1950s (Shephard et al., 1950; Sugawara et al., 2014; Tang & Weiss, 2015).

The mode of sediment transportation and deposition by tsunamis can be understood via a detailed study of tsunami deposits (Costa et al., 2015). Using this knowledge, a quantitative reconstruction of environmental conditions such as flow velocity and maximum flow depth has been attempted using several inverse modeling approaches (Johnson et al., 2017; Jerolmack & Paola, 2010; Ganti et al., 2014).

However, previous studies on inverse modeling were based on forward models using unreasonably simplified assumptions. For example, in the settling–advection model (or moving-settling tube model), it was assumed that all the sediment particles settle in the water column without any turbulent mixing, resuspension, or erosional processes (Soulsby et al., 2007; Moore et al., 2007; B. E. Jaffe & Gelfenbuam, 2007). Tang and Weiss (2015) assumed that the suspension in tsunamis occurs under uniform and steady conditions and inundation flows suddenly stop. As a result, situations to which these inverse models are applicable are quite limited (B. Jaffe et al., 2016; Naruse & Abe, 2017). Moore et al. (2007) proposed the point inverse model based on advection settings, wherein the settling velocities of the larger particles (D84 and D100) in the deposit were used as input data, and the model estimated the flow speed of the tsunami inundation. However, the travel distances of the grains were largely underestimated in this model because of the lack of resuspension processes. D. Smith et al. (2007) proposed another point model based on particle settlings but only the finest grain size classes of 106–184 μm were used in this model; however, the incorporation of larger grain size classses is essential for obtaining accurate estimation from tsunami deposits (Naruse & Abe, 2017). In contrast,

Soulsby et al. (2007) proposed the 1D model that deciphered the run-up elevation and inundation distance, although no resuspension, sediment dynamics and optimization of input parameters were considered. B. E. Jaffe and Gelfenbuam (2007) presented a point model (TsuSedMod) using suspended load as a formulation (Madsen et al., 1993) to reconstruct the maximum tsunami flow speed and vertical grain size distribution without considering the temporal variation of deceleration of the flow. This model overestimated the tsunami flow speed with uniform steady flow consideration in the formulations (Choowong et al., 2008). This model incorporates nonuniform and unsteady transport of suspended sediment and turbulent mixing; however, the FITTNUSS model still had many limitations. It employed a tedious trial and error method L-BFGS-B method, which is efficient quasi-Newtonian algorithm but it requires the gradient of the objective function that can be obtained only by numerical method. Also, it may find local minimum solutions depending on the starting values of calculation so that multiple iterations with different starting values are needed. As a result, it was difficult to deal with larger amount of data sets, and it was impossible to use uncertainty analyses because computational statistical methods, such as the jackknife method, require iterations of an inverse analysis.

In this study, we present a new inversion method comprising the use of a deep neural network (DNN) (Romano et al., 2009). This inverse model incorporates the same forward model used in FITTNUSS (Naruse & Abe, 2017). In this new methodology, however, the initial conditions and model parameters of the forward model are not optimized to fit the observed characteristics of tsunami deposits. Instead, the forward model calculation was simply repeated at random initial flow conditions (e.g., maximum inundation length, maximum flow depth, flow velocity, and sediment concentration) to produce artificial training data sets that represent artificial depositional characteristics such as the spatial distribution of thickness and grain size composition. The DNN was then trained to establish a relation between the characteristics of deposits and flow conditions based on artificial data sets. The established DNN can instantaneously predict the probable flow conditions from deposits, such that it works as an inverse model based on the tsunami deposits. The performance of the model was verified using training and test data sets. The efficiency verification of the model using data sets proved to be good results. Finally, this 1D model was applied to the 2011 Tohoku-Oki tsunami deposits from the Sendai plain, and a fair prediction of the flow velocity, maximum flow depth, and concentration of six grain size classes was obtained. The precision of the paleo hydraulics was also checked

using the jackknife method. The methodology and result were compared with the FITTNUSS model and the actual initial flow conditions. The comparison shows promising endorsement towards the use of DNN as a tsunami hazard assessment tool.

2 Model Formulation

This DNN inverse model primarily uses the forward model of FITTNUSS (Naruse & Abe, 2017), and the key feature of the new inverse model is that the model is implemented using an artificial neural network. The forward model calculates the sediment transportation and deposition from the averaged flow velocity, the maximum flow depth, and initial sediment concentration, and it produces a spatial distribution of the thickness and grain size composition, which are used to train the DNN inverse model.

2.1 Forward model

The FITTNUSS forward model is used in the present inverse model framework. Here, we describe about brief review of FITTNUSS forward model, and the details are presented in Naruse and Abe (2017). In the FITTNUSS model, shallow layer-averaged one-dimensional equations are used, which take the following form:

$$\frac{\partial h}{\partial t} + \frac{\partial Uh}{\partial x} = 0, \tag{1}$$

$$\frac{\partial Uh}{\partial t} + \frac{\partial U^2 h}{\partial x} = ghS - \frac{1}{2}g\frac{\partial h^2}{\partial x} - u_*^2. \tag{2}$$

where t and x are considered as the time and bed-attached streamwise coordinate which is, transverse to the shoreline and is positive towards the landward side. Here, h refers to the tsunami inundation depth, and U is the flow velocity. The gravitational acceleration is denoted as g, S is the bed slope and u_* is the friction velocity.

The sediment conservation equation of tsunami is given as follows:

$$\frac{\partial C_i h}{\partial t} + \frac{\partial U C_i h}{\partial x} = w_{si}(F_i E_{si} - r_{0i} C_i). \tag{3}$$

In the above equation, C_i refers to the volume concentration in the suspension of the ith grain size class. The parameters w_{si}, E_{si}, r_{0i}, and F_i represent settling velocity,

sediment entrainment coefficient, ratio of near-bed to layer-averaged concentration of the ith grain size class and volumetric fraction of the sediment particles in the bed surface active layer above the substrate respectively (Hirano, 1971). The closure equations for the above-mentioned equations include friction velocity (u_*), thickness of the active layer (L_a) (Yoshikawa & Watanabe, 2008), Shield's dimensionless shear stress (τ_{*m}), settling velocity (w_{si}) (Dietrich, 1982), sediment entrainment coefficient (E_{si}) (Rijn, 1984), correction of damping effects (ψ_i) (Rijn, 1984), For the sedimentation of tsunamis, the Exner equation of bed sediment continuity is used:

$$\frac{\partial \eta_i}{\partial t} = \frac{1}{1-\lambda_p} w_{si}(r_{0i}C_i - F_i E_{si}). \tag{4}$$

Here η_i refers to the volume per unit area (thickness) of the sediments of the ith grain size class which includes porosity of the bed sediment λ_p. As a result of the sedimentation, the grain size distribution in the active layer varies with time (Hirano, 1971), which is expressed as follows:

$$L_a \frac{\partial F_i}{\partial t} = \frac{\partial \eta_i}{\partial t} - F_i \frac{\partial \eta}{\partial t} \tag{5}$$

Thus, the rate of total sedimentation is as follows:

$$\frac{\partial \eta}{\partial t} = \sum \frac{\partial \eta_i}{\partial t}. \tag{6}$$

Equations (4) to (6) were solved using the two step Adams–Bashforth scheme and the predictor-corrector method. Finally, the the flow dynamics of tsunamis was simplified using the assumption proposed by (Soulsby et al., 2007), while considering velocity of tsunami run-up flow as uniform and steady but that the flow depth varies with time; thus, the model is based on quasi-steady flow assumption. The simplified equation is as follows:

$$\frac{\partial C_i}{\partial t} + U\frac{\partial C_i}{\partial x} = \frac{R_w}{H\,(Ut-x)} \left\{ w_{si}\left(F_i E_{si} - r_{0i}C_i\right) \right\}. \tag{7}$$

where R_w and H indicate maximum inundation length and Maximum flow depth of the tsunami at the seaward (upstream) boundary of the transect, respectively.

In addition to these formulations, a transformed coordinate system (Crank, 1984) has been applied to equation (7) to increase the computational efficiency of the forward model. The implicit Euler method was used to solve the equation after applying coordinate transformation. The entire forward and inverse model were implemented using Python with the Numpy and Scipy libraries.

2.2 Inverse model

Although artificial neural networks have been primarily applied for learning observational data sets for constructing predictive models (Ramirez et al., 2005), in this study, they are used for learning the results of a numerical simulation to construct an inverse model. First, artificial training data sets are prepared by repetition of the forward model calculation with random initial and boundary conditions. The data set comprising the spatial distribution of the grain size composition (Figure 1) is given to an input layer of the NN. The nodes in the input layer receive the values of the volume per unit area of each grain size class at the spatial grids used in the forward model. The feed-forward calculation through several hidden layers is then performed, in which the values at the nodes were summated with weighting coefficients that are assigned on connections to nodes in the next layer, and the computed total input data passes through the activation functions to produce the net output. The number of hidden layers was set to maximize the model performance (S. Smith, 2013). As a result of this feed-forward calculation, the values obtained from the output nodes provide estimates of the hydraulic conditions of tsunamis that formed the deposits. This procedure results in the training of the model followed by testing of the model performance. The 20% of the artificial data is used to validate the model performance during training. If the model tends to overlearn, the selection of hyperparameters and the optimization method is required to be revised. After the model training is completed, the model is ready for application to a natural data set; however, the model performed training based on artificial data with a definite spatial grid interval.

2.2.1 Procedures for training of the inverse model

Here, we describe the procedures used for generating a training data set and the preprocessing. In the present study, in the forward model, the grain size distribution was discretized into six grain size classes, and the number of spatial grids in the transformed

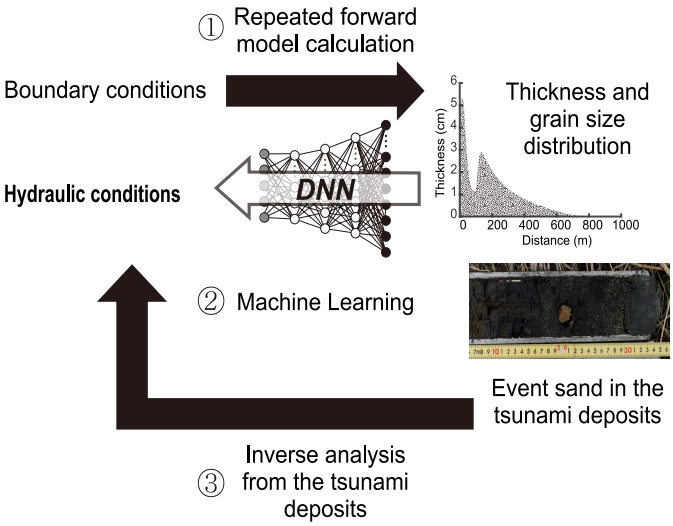

Figure 1. Workflow of the DNN inverse model.

coordinate was 50. The number of spatial grid sizes in the fixed coordinates depends on the size of the sampling window, as mentioned previously. It is important to determine the appropriate number of training data sets produced by the forward model in order to improve the inverse model training (Jordan & Rumelhart, 1992). In this study, the number of iterations of the forward model calculation was incrementally increased, and the relation between the number of training data sets and the performance of the inverse model was investigated. The range of the explored conditions in the training data set is described later. The sampling window was then set to the artificial training data sets before starting the training of the DNN, and only the data in the sampling window was used for the training. This sampling window was necessary because (1) the thickness of the collected samples at a distant location becomes too thin to measure precisely and predict computationally, and (2) the measurement transect cannot cover the entire distribution of the tsunami deposits in natural cases. Very thin and fine-grained tsunami deposits in the distal area may not be differentiated from the background soil, and thus, the region of analysis should be limited to a relatively proximal area wherein coarse and thick-bedded deposits are distributed. Therefore, the specific window is preferably at the proximal to middle part of the transect. As in the settings of our inverse model, the grid spacing has been maintained at a constant value and measures 15 m in our model. The number of spatial grids in the fixed coordinate varies according to the selected interval

of the sampling window. After the production of the training data set and extraction of the sampling window, the normalization of the input and teacher values was performed, which is one of the most important processes in training the neural network. As the input and teaching data have largely a different range of values from each other, the normalization of the values is required to be performed to remove the computational biases towards a specific dimension of data (Bishop et al., 1995). In this case, the maximum inundation length has a larger range of values, while the values of concentration are very low. Thus, the raw values of the teaching data may predict the inundation length preferentially, while the concentration values tend to be ignored. Therefore, both the input and teaching data in the artificial data set produced by the forward model were normalized before they were given as input to the inverse model. The input data (volume per unit area of deposits) were normalized using the following equation:

$$X_{norm} = (X_{raw} – min\, val_{X_{raw}}/(max\, val_{X_{raw}} - min\, val_{X_{raw}}) \tag{8}$$

where X_{norm} and X_{raw} are the normalized and original values of the input data respectively. $min\, val_{X_{raw}}$ and $max\, val_{X_{raw}}$ denote the minimum and maximum values of the raw input data, respectively. Similarly, the teaching data that was the original conditions used in the forward model calculation was normalized using the following equation:

$$Y_{norm} = (Y_{raw} – min\, val_{Y_{raw}}/(max\, val_{Y_{raw}} - min\, val_{Y_{raw}}) \tag{9}$$

where Y_{norm} and Y_{raw} are the normalized and original values of the teaching data respectively. $min\, val_{Y_{raw}}$ and $max\, val_{Y_{raw}}$ denote the minimum and maximum values respectively, of raw teaching data. After the training, the NN outputs the normalized values of the hydraulic conditions, such that these values were converted to values in the original scale.

Then, the training and teaching data set were given to the NN for training. The overall neural network structure consists of three parts, the input layer, hidden layers, and output layer (Figure 3). In the inverse model, the input layer of neural network structure consists of input nodes where the input values comprise the volume per unit area of each grain size class at the spatial grids. Thus, the number of input nodes can be expressed as $M \times N$ where M and N are the total number of spatial grids and grain size

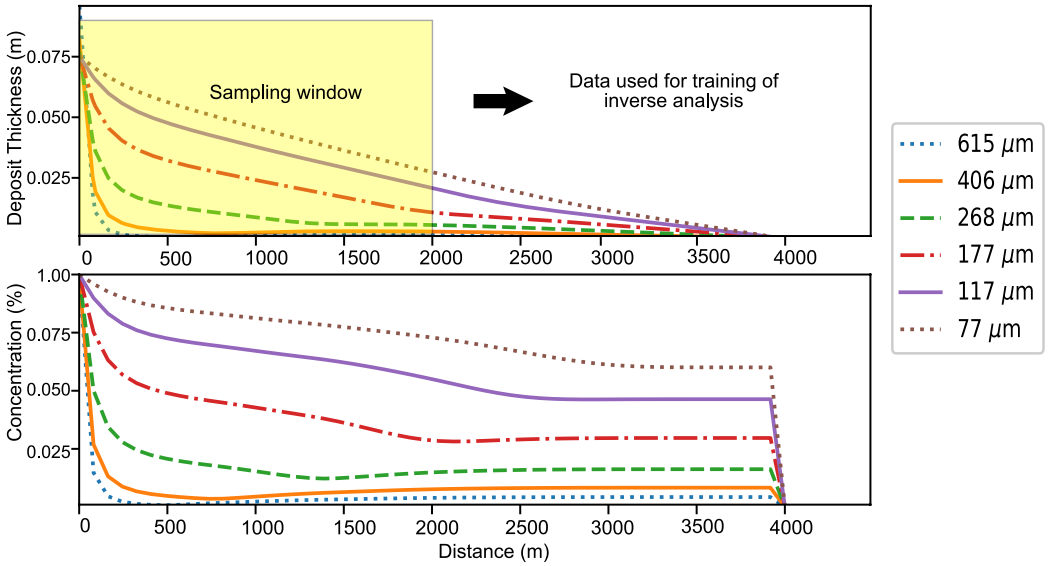

Figure 2. Example of the forward model calculation and sampling window used for the inverse analysis. (a) Spatial variation of the volume per unit area of each grain size class of the tsunami deposit calculated using the forward model (b) Spatial variation of sediment concentration of each grain size class in the run-up flow when the flow has reached the maximum inundation point.

classes respectively. In this study, the number of dense hidden layers was set as three along with the total 2500 nodes, and thus total number of layers was five (Figure 3). Here, the rectified linear activation function (ReLU) was used as an activation function that calculates the output value from the total net weighted inputs (Ian & Yoshua, 2016). ReLU is function that is widely used for this purpose (Patterson & Gibson, 2017). The drop out has been applied to the hidden layer for regularization of the NN (Srivastava et al., 2014). The results of the feed-forward calculation of this NN during the training process were evaluated by the loss function (mean squared error), which is defined as follows:

$$J = \frac{1}{2}\sum\left(I_k^{fm} - I_k^{NN}\right)^2 \tag{10}$$

where I_k^{fm} is denoted as the teaching data that are the initial parameters used for producing in the training data and I_k^{NN} denotes the predicted parameters. This loss function quantifies how close the NN was to an ideal inverse model. The values of this func-

tion were averaged over the entire data set (Patterson & Gibson, 2017). To minimize the loss function J, the back-propagation method with the stochastic gradient decent algorithm (SGD) was used to optimize the weight coefficients at links of the network (Patterson & Gibson, 2017). The nesterov momentum was used with the SGD to speed up the computation and improve convergence (Sutskever et al., 2013). Although other optimizers such as AdaDelta, Adam, or AdaMax can provide an acceptable performance (Patterson & Gibson, 2017), this optimizer was showing best performance in case of our model. This optimization process was repeated for prescribed times, and the training set was shuffled before splitting it into batch chunks that were used for the SGD optimization during each epoch.

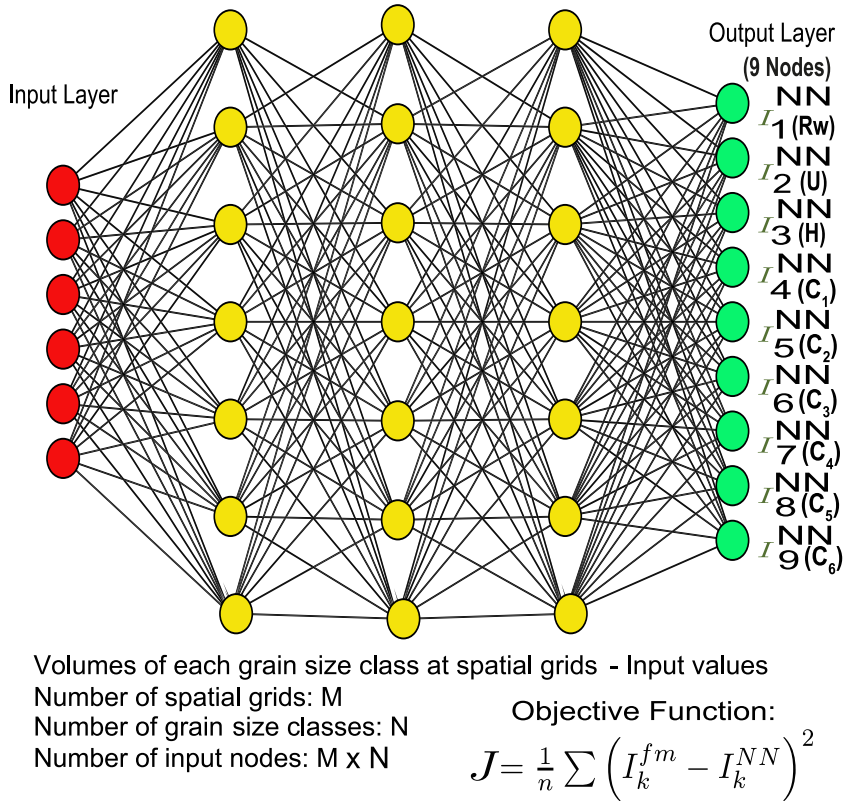

Figure 3. NN architecture for the inverse model. The NN structure includes one input and one output layer with three hidden layers and a total of five layers.

In order to estimate how well the model was trained without overfitting, validation was performed with the validation data set that was also generated from the for-

ward model calculation. Among the produced data sets, 80% and 20% of the data were used for the training and validation respectively. The results of validation were used for tuning of the hyperparameters which are explained later. Finally, the performance of the model was evaluated after the hyperparameter tuning and using the test data sets, which comprised the unused data set during the training process.

In our model, there are several hyperparameters that should be specified for the tuning of the training of the NN. The tuned hyperparameters were the learning rates, batch size and momentum used in the SGD, rates of drop out, number of hidden layers, types of activation function, and number of epochs. The hyperparameters were selected by trial and error in this study. The number of training data sets is also a hyperparameter of the inverse model, and it was tested by changing the number of repetitions of the forward model calculation. The trained model can work on a data set with a specific spatial grid in the fixed coordinate and grid spacing. In order to apply the inverse model to the natural data set in 1D vectors, the collected samples must be fit into that fixed coordinate. A linear 1D interpolation was required as it provides values at positions between the data points, which are joined by straight line segments (Bourke, 1999). A linear 1D interpolation was applied to the natural data set in this case.

In addition to the training and validation data, 500 independent data were kept aside for the testing of the inverse model. Therefore, after the model was trained, the model was applied to the test data sets to check its performance before applying it to the natural data sets. The correlation between the teaching data in the test data set and the prediction of the model from the test data set was used to determine the precision and accuracy of the inverse model prediction. The residuals from the teaching data in the test data set were plotted in a histogram to determine the deviation of the prediction from the test data set from the true initial conditions.

2.2.2 Uncertainty analysis of inversion results

The jackknife method was used for the error assessment of the results of the inverse model. This method estimates the standard error of the predicted value of the model using a resampled population. Quenouille (1949) first introduced this resampling method (Nisbet et al., 2009).

The jackknife test is similar as the bootstrap method, but instead of a random sampling of a data set, the inversion model works on each separate set of samples by omitting a single set of observations per iterations from a total of N observations. Inversions are carried out N times and the resulting ensemble of solutions were interrogated to a single estimate for each parameter. In short, it involves a leave-one-out strategy in a data set of N observations and the model works on the rest of the samples and gives results accordingly. Preferably, $N-1$ observations were built on the data set as resampled data for the model. Farrell and Singh (2010) discussed the importance of the jackknife method in survey sampling.

We briefly describe the jackknife uncertainty analysis. The estimate from a sample and the jackknife estimates are denoted as S and S^* respectively. The number of observations in the sample is N and the set of observations is denoted as $\{X_1, ..., X_n, ..., X_N\}$. The sample estimate of the parameter acts as a function of the observations in the sample (Abdi & Williams, 2010). The equation is given as follows:

$$S = f(X_1, ..., X_n, ..., X_N) \tag{11}$$

Let S_{-n} be the $n-$th partial prediction of the parameter, which is produced by the inverse model without the nth observation. The equation for the prediction S_{-n} is given as follows:

$$S_{-n} = f(X_1, ..., X_{n-1}, X_{n+1}..., X_N) \tag{12}$$

S_n^* represents a pseudo value estimation of the nth observation. This parameter is defined as the difference between the estimates S obtained from the entire sample and the estimates S_{-n} obtained without the nth observation as follows:

$$S_n^* = NS - (N-1)S_{-n} \tag{13}$$

The mean of the pseudo values are regarded as the jackknife estimate S^*. The equation for the jackknife estimate is given as follows:

$$S^* = S^*_{mean} = \frac{1}{N}\sum_{n}^{N} S^*_n \tag{14}$$

where S^*_{mean} is also the mean of the pseudo values. The variance of the pseudo values is denoted as σ^{var}_{JK} and the formula for the variance is given as follows:

$$\sigma^{var}_{JK} = \frac{\sum (S^*_n - S^*_{mean})^2}{N-1} \tag{15}$$

Finally, the jackknife standard error of the parameter estimate is denoted as σ^{SE}_{JK}, The formula for the jackknife standard error is

$$\sigma^{SE}_{JK} = \sqrt{\frac{\sigma^{var}_{JK}}{N}} = \sqrt{\frac{\sum (S^*_n - S^*_{mean})^2}{N(N-1)}} \tag{16}$$

The confidence interval for this study has been computed using this jackknife standard error formula.

3 Results of training and test of the inverse model

The hyperparameters for the training were set as follows. Among the hyperparameters used in the SGD algorithm, the learning rate was set as 0.02 and batch size was kept as 32 for our models (Patterson & Gibson, 2017). The use of larger or smaller learning rates did not provide improved results. Furthermore, other batch sizes were used in the training of the model, but the model was not improved. The selection of number of layers and the number nodes were tested by increasing or decreasing layers or nodes, and finally three hidden layers with 2500 nodes were used in the models. Another hyperparameter is the rate of drop-out at each hidden layer, which was 50% in our model. Thus, during the training, 50% of the layer outputs that were randomly selected were kept inactive. This regularization process helps to reduce overfitting and increases the efficiency of the training (Srivastava et al., 2014). Finally, the number of epochs in the training process, which indicates number of times that a full data set has passed the optimization calculation (J. Smith & Eli, 1995), were determined depending on the rates of the progress of the training (Figure 4). This is described in the following sections.

The input parameters for the inverse model include the maximum inundation length, flow velocity, maximum flow depth, and the sediment concentration of six grain size classes.

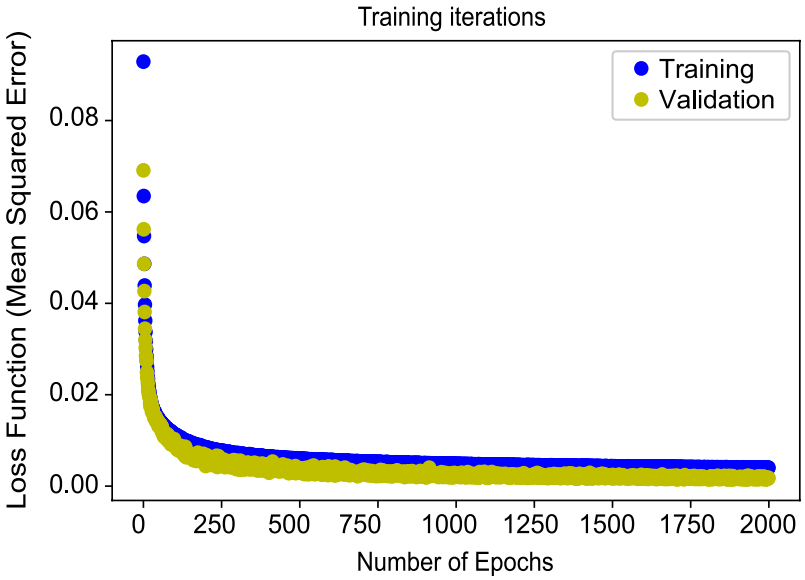

Figure 4. History of learning indicated by the variation of the loss function (mean squared error). Both the values of the loss function for the training and validation data sets decrease over 2000 epochs without any discrepancy, thus indicating that overlearning did not occur.

The range of values for the maximum inundation length, flow velocity, maximum flow depth, and sediment concentration used for generating the training data sets were 2500 to 4500 m, 1.5 to 10 m/s, 1.5 to 12 m, and 0 to 2%, respectively. The values of the loss function of the training and validation at the first epoch were 0.0929 and 0.0691 for the training and validation data, respectively. These values are based on the maximum records of tsunamis in the studies of Mori et al. (2012), Nakajima and Koarai (2011), Foytong et al. (2013), B. E. Jaffe et al. (2012).

The values of the loss function of training and validation at the first epoch were 0.0929 and 0.0691 for the training and validation data, respectively. The value of the loss function decreased to less than 0.01 after 200 epochs. The present model was reasonably converged over 2000 epochs for both the training and validation performance, which remained in unison and equivalent. Moreover, the plot for the loss function was smooth, and there was no anomalous oscillation. The last and lowest loss function at the final epoch was 0.0040 for the training data sets and was 0.0018 for the validation data sets. The sampling window was set from 0 to 2000 m in this training and the following tests (Figure 2).

For the current inverse models, the forward model was calculated repeatedly from 500 to 4500 iterations, and it provided the best result with 4500 iterations of calculations of the forward model (Figure 5). Figure 5 presents a plot of the relation between the number of training data and loss function of the validation data set. The loss value of the validation data set decreases as the amount of training data increases, which creates concave-upward shape. When the number of training data in the data set was 500, the loss function was higher but decreased significantly after 1500 training data sets. The loss function reached a minimum value after 3500 training data sets and did not change much subsequently. Thus, it was suggested that the number of training data sets should be greater than 3500. The number of training data sets thus used was 4500.

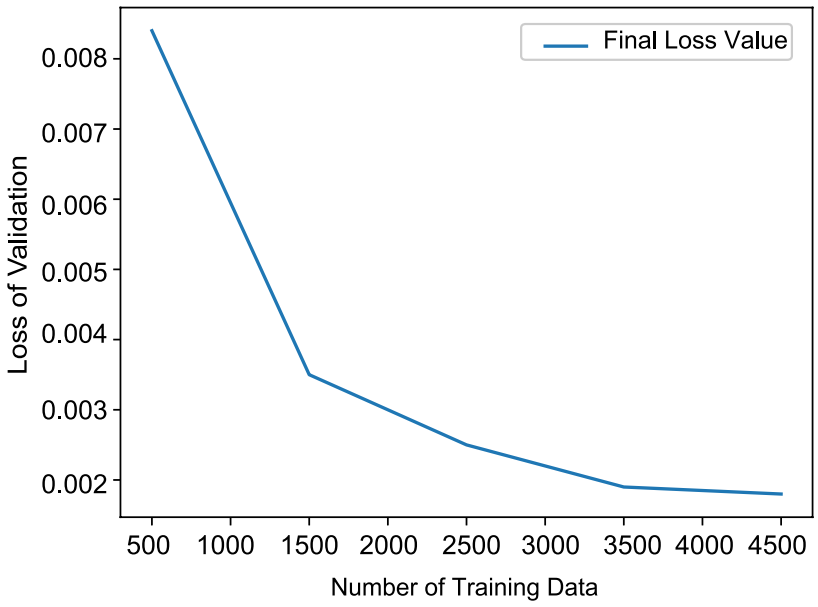

Figure 5. Relation between the loss function of the validation and number of training data sets selected for the inverse model. The results of the training improved as the number of training data sets increased, whereas it varied slightly after 4000 training data sets.

After the training of the model, the prediction results of the inverse model from the test data sets were plotted against the original conditions used for producing the test data sets. Figure 6(a-i) shows that the nine predicted initial conditions from the artificial test data sets were distributed along the 1:1 line in the graph, thus indicating that the test results showed a correlation with the true initial conditions. Furthermore, the residuals of the predicted parameters from the true initial conditions were plotted on a

histogram to show the distribution of the deviation of the test results from the original conditions.

Figure 7(a-i) shows that the deviation of the parameters predicted from the original values were distributed in a relatively narrow range without large biases from the true conditions, except in the case of the maximum flow depth. Only the maximum flow depth was slightly biased. Based on the scatter diagram (Figure 7), the values of the predicted maximum flow depth were approximately 0.5 m lower than the original value.

4 Result of application to the 2011 Tohoku-Oki tsunami deposit

The model was applied to the 2011 Tohoku -Oki Tsunami deposits distributed around the Sendai plain for the evaluation of the models. This region was extensively surveyed for hazard evaluation as well as tsunami deposits (Naruse & Abe, 2017; Abe et al., 2012), and thus, large amounts of field data are available for evaluating the inverse models. In this study, the field data used was the same as that used for the FITTNUSS model (Naruse & Abe, 2017), and therefore the inversion methodology can be compared with the previous study.

4.1 Field description and settings for inverse analysis

We briefly describe the field sampling method for the measured data. The field work for obtaining these tsunami deposits was conducted soon after the tsunami event in June 2011 (Naruse & Abe, 2017), and the details can be referred to in the studies of Abe et al. (2012) and Naruse and Abe (2017). The study area (Figure 8) mainly consists of a long sandy beach, high onshore seawall, aeolian sand dunes, coastal forests, and long flat rice-paddy fields successively towards the landward side (Naruse & Abe, 2017). The deposit samples were obtained every 50–100 m at 26 sites along the transect. The thickness of tsunami sand and mud layers ranged from 0.1 cm to 34 cm. The grain size analysis of the tsunami deposit showed that the tsunami sand mostly comprised medium sand with a small presence of fine and very fine sand (Naruse & Abe, 2017). The measured grain size distributions were then discretized to six grain size classes (Figure 9), while the previous FITTNUSS model employed four grain size classes (Naruse & Abe, 2017). The representative diameters of the grain size classes were 615, 406, 286, 177, 117 and 77 μm respectively.

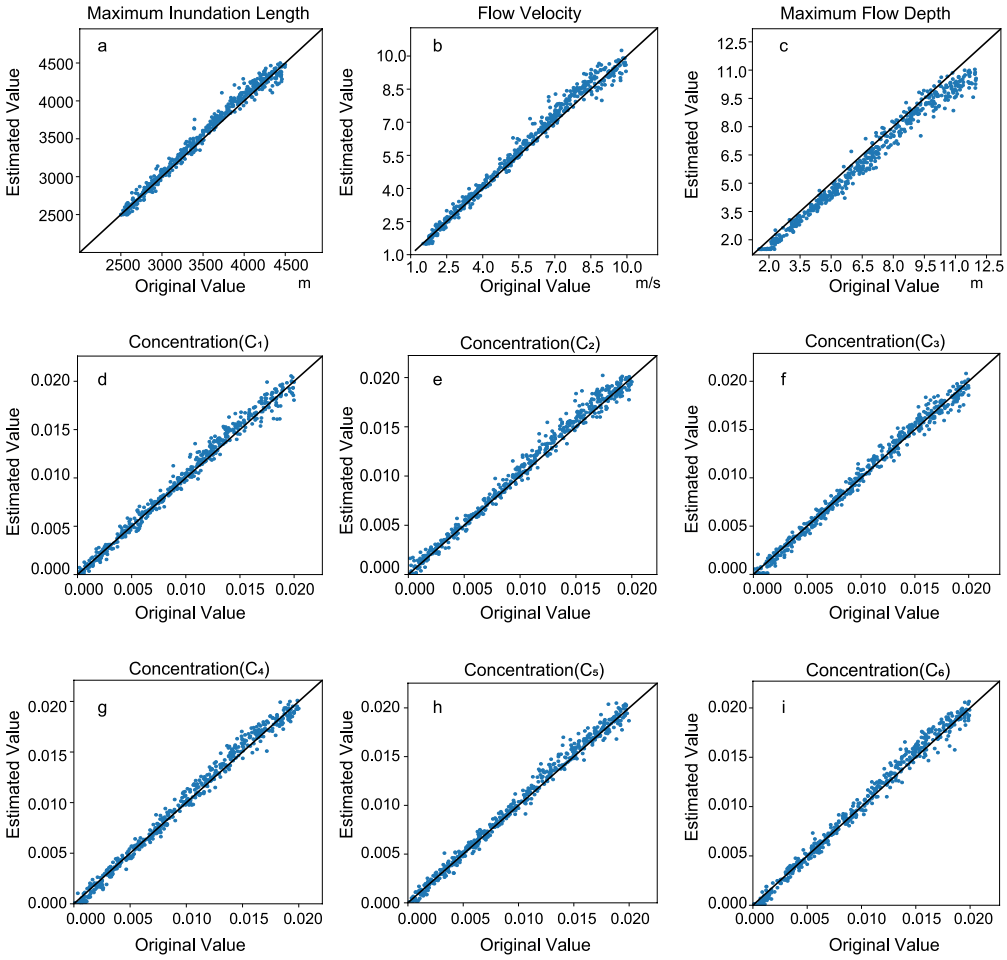

Figure 6. Verification of the performance of the model using artificial test data sets. The values estimated using the inverse model were plotted against the original values used for the production of the test data sets. The solid lines indicate a 1:1 relation and suggest precise estimation.

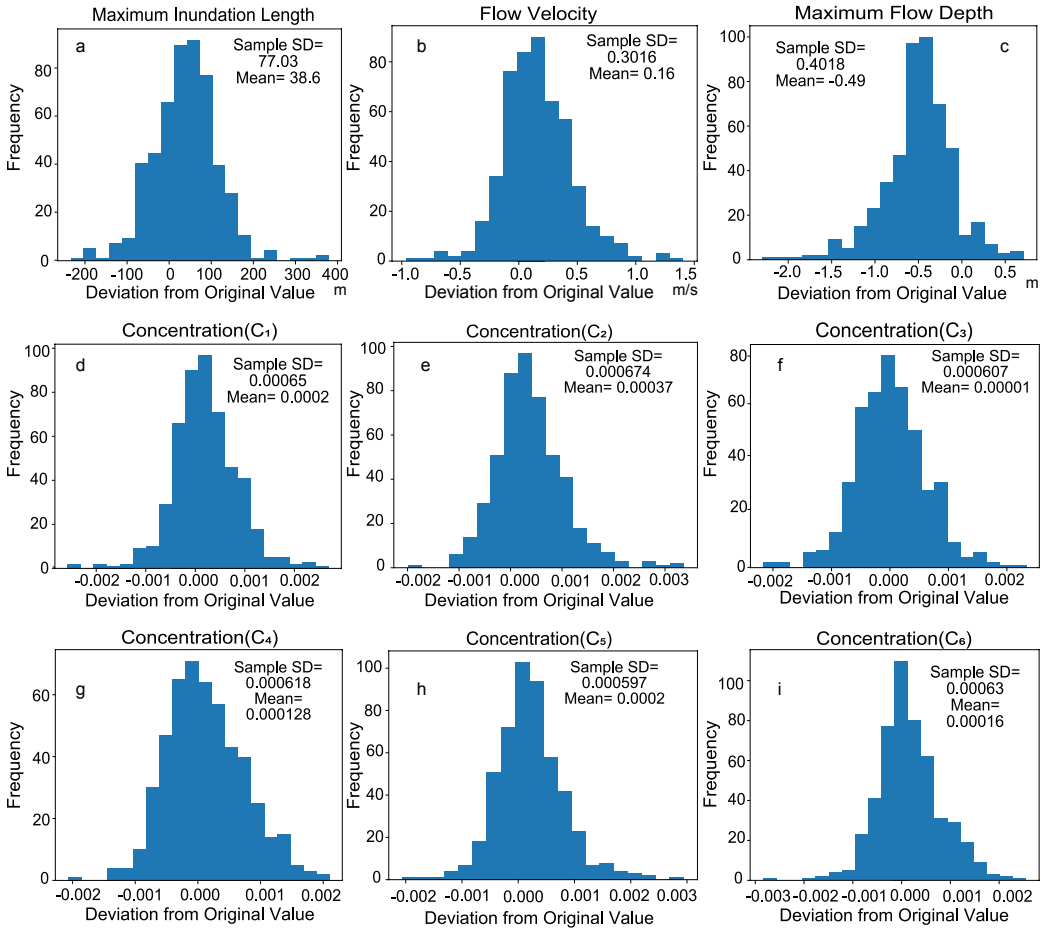

Figure 7. Histograms show the deviation of the predicted results from the original values of the artificial test data sets.

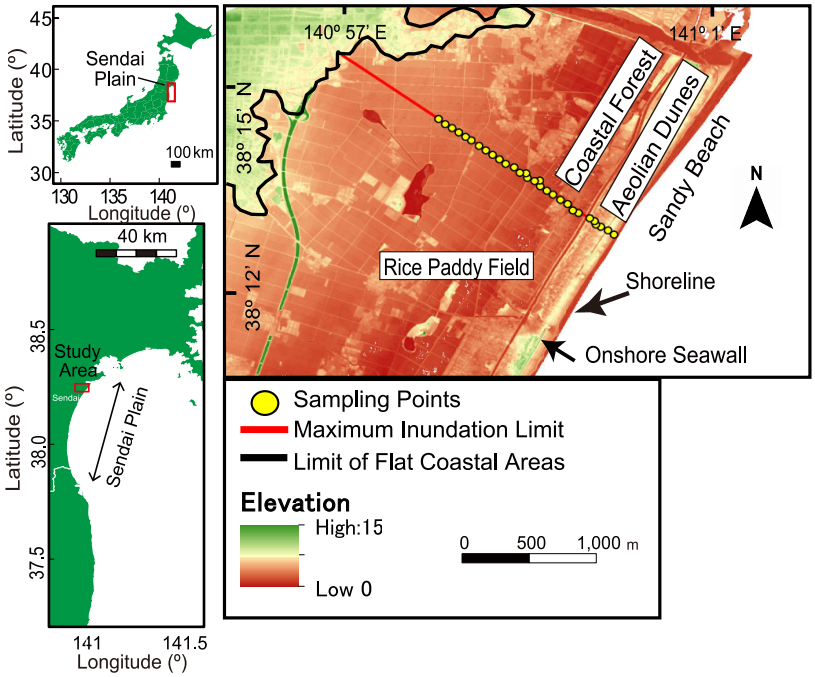

Figure 8. Location of the survey transect and sampling points on the Sendai plain. The location of the surveyed transect is shown on the topographic map of the study area. The 4 km long transect was situated transverse to the shoreline, and the tsunami deposit was sampled at 27 locations along the transect (Naruse & Abe, 2017).

The parameters such as the flow velocity estimated using the inverse model were verified by comparing them with the data obtained from aerial videos and observations of the Sendai plain (Hayashi & Koshimura, 2013; Mori et al., 2012). Although it is difficult to assess sediment concentration data obtained from direct field observation, Goto et al. (2014) roughly estimated the sediment concentration in the tsunami inundation flow based on the ratio of the deposit thickness and flow height. We compared our reconstruction of the sediment concentration with their results.

4.2 Determination of length of sampling window

In this case, the sampling window was set at a region from 0 to 2000 m along the transect. Although the total distance of the transect for collecting the samples was approximately 3000 m, the measured bed thickness was very thin (several millimeters) and exhibited a large fluctuation in the distal region (2000 to 3000 m) (Figure 12). There-

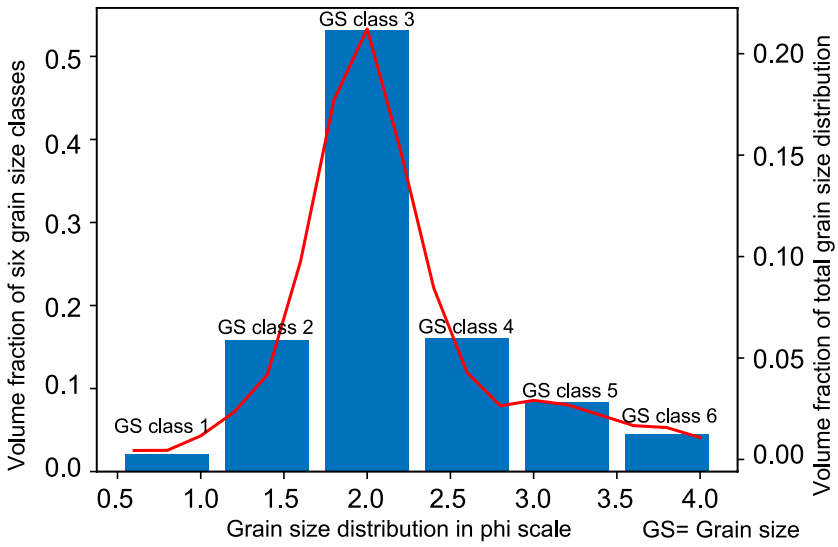

Figure 9. Total grain size distribution of the tsunami deposits in the Sendai plain and the discretized fraction of the sediments in the six grain size classes.

fore, a 2000 m long sampling window was extracted from the sampling distance, which is 3000 m. This size of sampling window was also used for training the inverse model. For this situation, the number of spatial grids used for the inversion was 133 because the grid spacing in the fixed coordinates was 15 m. The selection of a sampling window of this size was checked based on a comparison with the results obtained using different sampling windows, and the results of the comparison suggested that 2000 m was the most suitable for obtaining stable results. Figure 10 shows the fluctuations of the jackknife standard error estimation of the parameters depending on the sampling window sizes. The majority of the parameters such as flow velocity and sediment concentrations exhibited a decreasing trend in their estimation errors as the length of the sampling window was increased. In particular, the jackknife error of the flow velocity decreased significantly above a sampling window size of 1000 m in length. The estimates of the maximum inundation length show large errors but it decreased suddenly at approximately 2500 m. In contrast, the error in the maximum flow depth increased above a sampling window size of 2000 m. Hence, it was decided that the size of the sampling window was set as 2000 m. It should be noted that the computation result for the maximum inundation length was unstable at this selection.

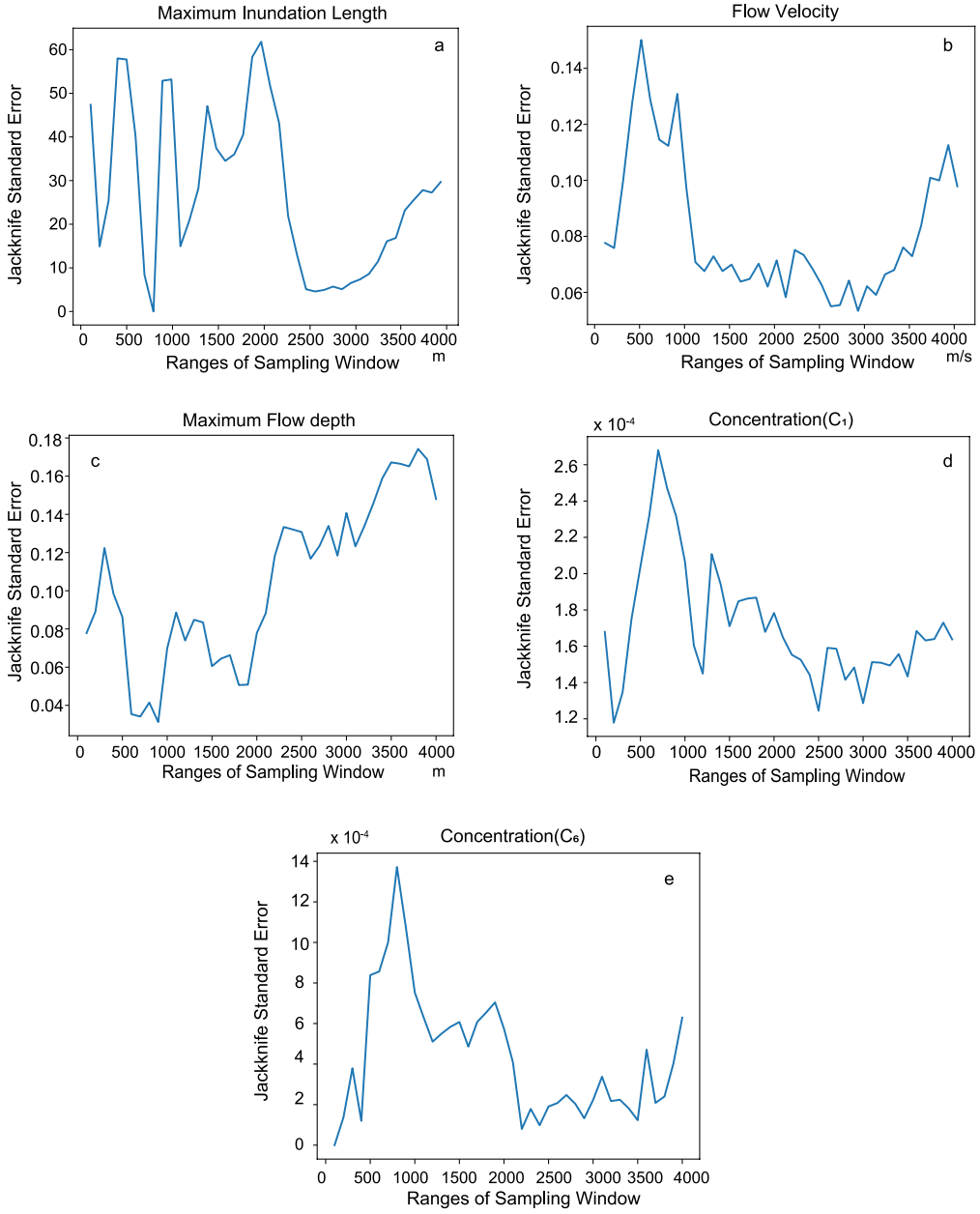

Figure 10. Variation of jackknife standard error with changing range of sampling window distance.

Table 1. Predicted results by inverse model applied to 2011 Tohoku-Oki tsunami deposit data obtained from Sendai plain

Parameters	Predicted Results	Confidence Interval (95%)
Maximum Inundation Length	4045 m	± 121.17 m
Flow Velocity	5.4 m/sec	± 0.140 m/sec
Maximum Flow Depth	4.11 m	± 0.152 m
Concentration of C_1 (615 μm)	0.55%	± 0.034%
Concentration of C_2 (406 μm)	2.19%	± 0.048%
Concentration of C_3 (268 μm)	1.98%	± 0.058%
Concentration of C_4 (177 μm)	0.14%	± 0.018 %
Concentration of C_5 (117 μm)	0.18%	± 0.012%
Concentration of C_6 (77 μm)	0.04%	± 0.0011%

4.3 Result of inversion

The inverse model reconstructed the flow conditions of the tsunami from the deposit of the 2011 Tohoku-Oki tsunami in the Sendai plain. The model estimated flow parameters that were close to the observed values.

Table 1 shows the predicted hydraulic conditions of the 2011 Tohoku-Oki tsunami of the Sendai plain. The predicted result of the flow velocity was approximately 5.4 m/s with a range of uncertainty ± 0.140 m /sec using jackknife standard error calculation with a 95% confidence interval (Figure 11b). The value of the maximum flow depth was appoximately 4.11 m (± 0.152 m uncertainty using jackknife standard error calculation (Figure 11c) with a 95% confidence interval).

The reconstructed total sediment concentration over six grain size classes was 5.08%. The estimated value of the sediment concentration of each grain size class ranged from 0.04% to 2.19% (Figure 11d-11i).

The model predicted the maximum inundation length of the tsunami from the deposit, as approximately 4045 m with a ± 121.17 m jackknife standard error with a 95% confidence interval (Figure 11a). The actual inundation length was 4020 m (Naruse & Abe, 2017), which is consistent with the reconstructed value.

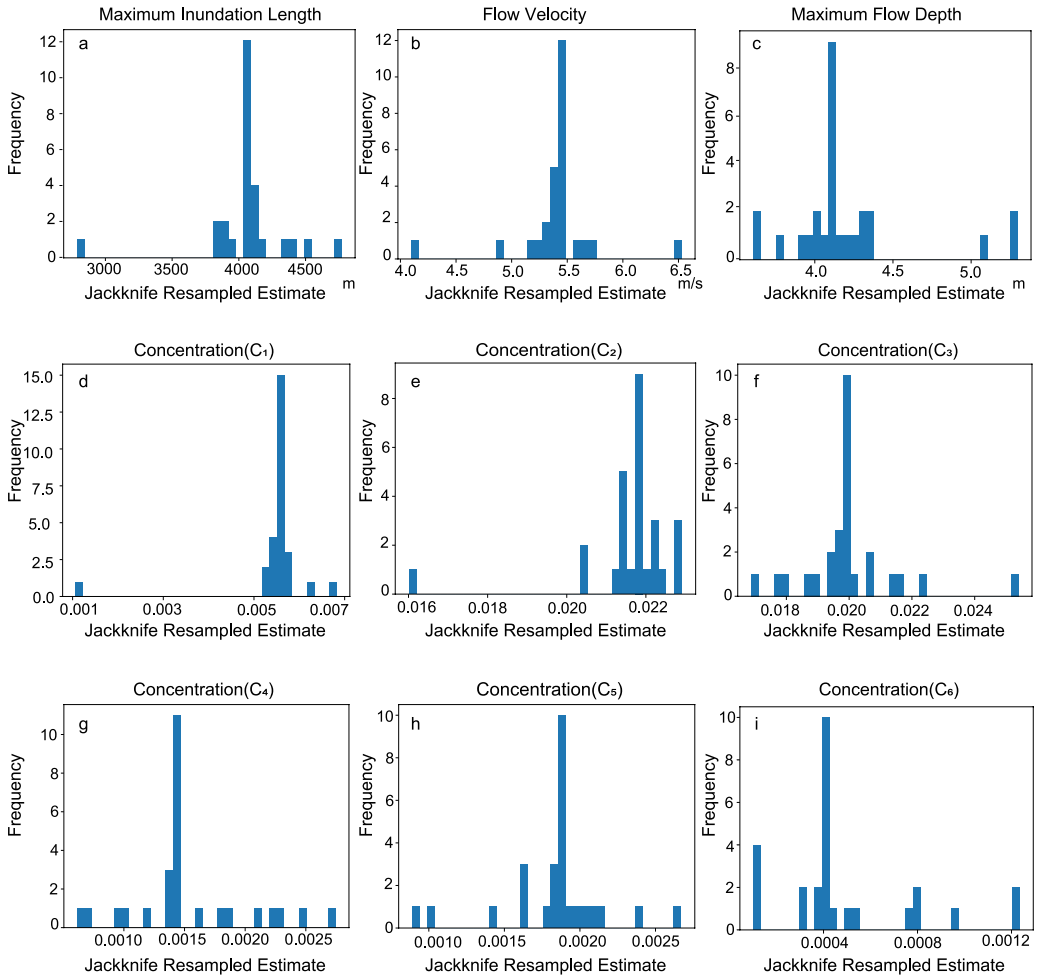

Figure 11. Jackknife estimates for the results predicted by the inverse model to determine the uncertainty of the model.

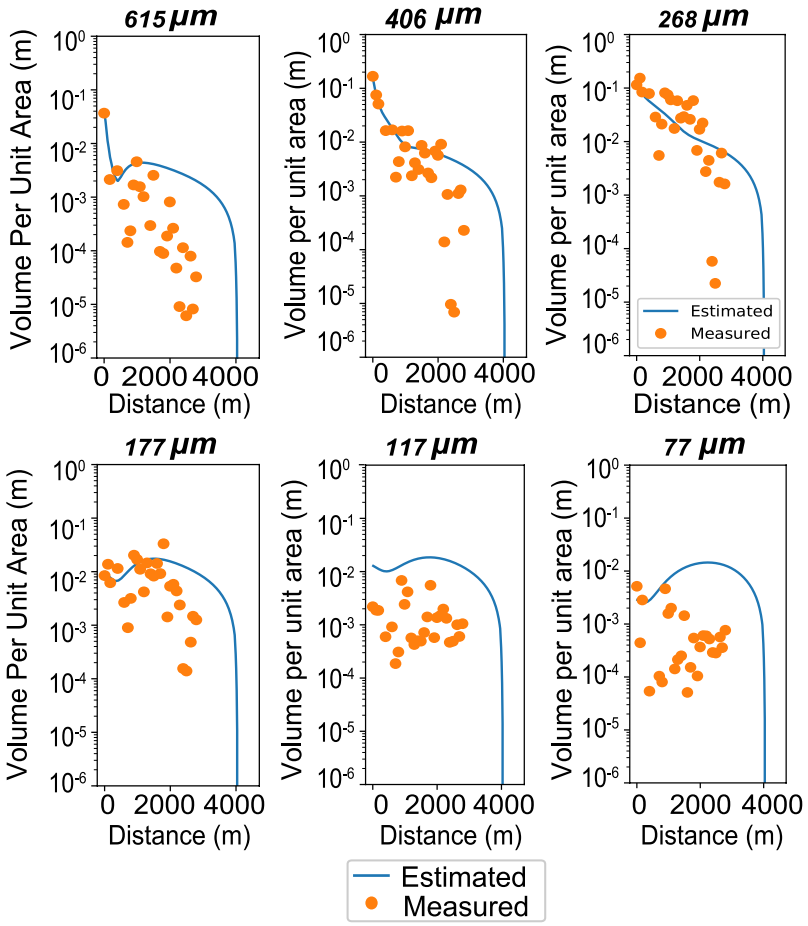

Figure 12. Spatial variation of the thickness of the tsunami deposit. Spatial distribution of volumes per unit area of six grain size classes is presented. The solid circles indicate the values measured by Naruse and Abe (2017), and the lines indicate the results of the forward model calculation obtained using parameters predicted by the inverse model.

For the error assessment of model results, the jackknife method was used. In this method the standard error and variance is estimated from a large population (Nisbet et al., 2009).

Finally, using the reconstructed initial conditions of the tsunami, the forward model was used to calculate the spatial distribution of the thickness and grain size composition for a comparison with the measured distribution. Figure 12 exhibits the thickness and grain size distribution with the distance for the measured data and simulated results. The measured values of volume per unit area for each grain size class matched the

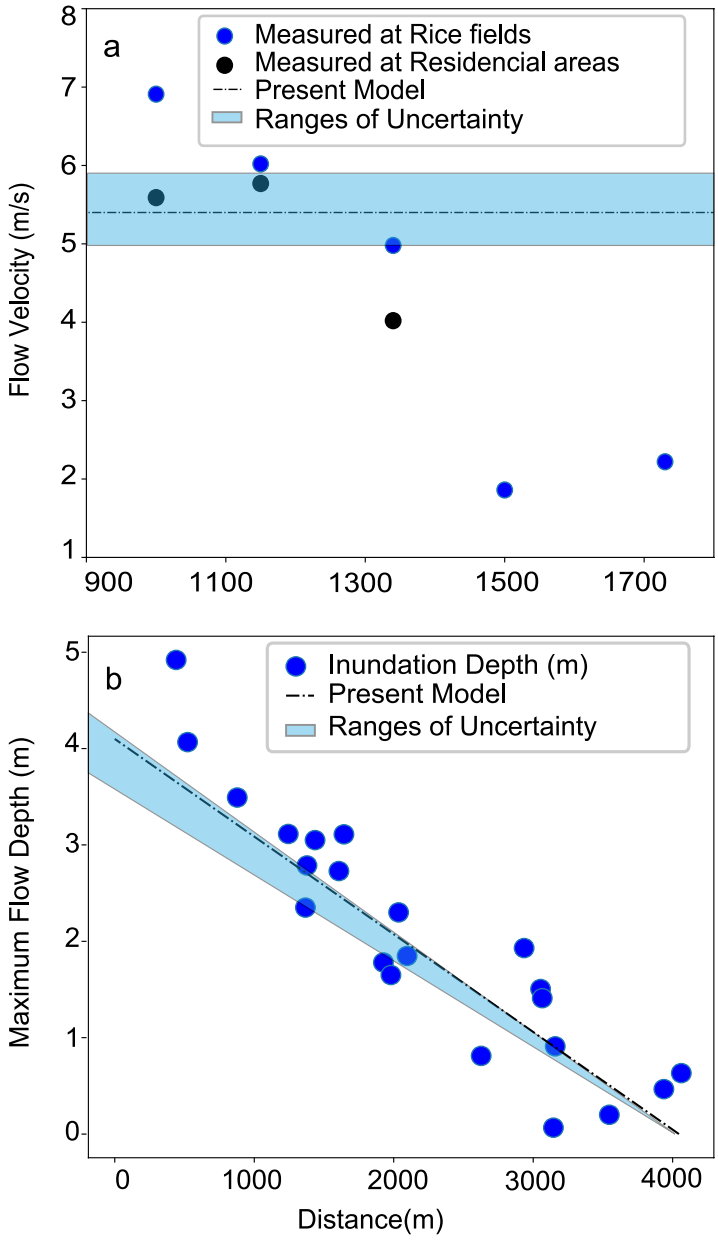

Figure 13. Comparison between field observation and results of inverse analysis of 2011 Tohoku-Oki tsunami. The solid dots are measured values by field observation, and the lines are results of the inverse analysis of this study. (a) Velocity of run-up flow of the 2011 Tohoku-Oki tsunami on Sendai plain. (b) Maximum flow depth of 2011 Tohoku-Oki tsunami on Sendai plain. Values measured from the aerial videos are indicated by the solid and open circles (Hayashi & Koshimura, 2013), and the results of the inverse analysis are shown by the lines.

simulated results except in the case of the finest grain size class, where the predicted values were larger than the actual measurements.

5 Discussion

5.1 Tests of inverse models

The tests of the inverse models performed using the artificial data sets of tsunami deposits demonstrated that the models built using NN can predict the flow velocity and the concentration of six grain size classes, maximum inundation length precisely. The scatter diagram of the predicted parameters against the true conditions indicates excellent correlation (Figure 6). For example, 2σ of the estimation error of the maximum inundation length was 121.17 m, and the range of true values was 2500–4500 m (Figure 11). Thus, the precision of estimates is only the order of approximately 5%. More importantly, there was no large deviation of mode of predicted values from true conditions except for the maximum flow depth. Especially in cases of estimates of sediment concentration, mean of the estimation errors ranges within 1.0×10^{-3}. These lines of results imply that the prediction of the inverse model is precise and accurate.

However, the model tends to estimate maximum flow depth values that are approximately 0.5 m higher. As a result, in the comparison of the predicted values and original values of the maximum flow depth plotted in the histogram, the deviation shows a positive bias, and the mode value was approximately 0.5 m towards the negative side. Despite the skewness, it is possible to correct the final result of the maximum flow depth by adding 0.5 m with the final reconstructed value from original field data.

5.2 Reconstruction of the flow parameters of the 2011 Tohoku-Oki tsunami

After applying the inverse models to the 2011 Tohoku-Oki tsunami, the predicted results of the flow velocity and the inundation depth were close to the values observed in the aerial video and field measurements (Figure 13), which indicates the effectiveness of the proposed method in applying the actual tsunami deposits.

Figure 13 shows that the averaged value of the observed inundating flow velocity of 2011 Tohoku-Oki tsunami ranged from 4.8 to 5.8 m/s, and the reconstructed values are in this range.

The predicted inundation length was 4045 m which is very close to the original maximum inundation length of approximately 4020 m. Furthermore, the model predicted the concentration of six grain size classes satisfactorily. The range of the estimated concentration for each grain size class was 0.04–2.19 vol.%, and the total concentration was 5.08 vol.%. There has been no direct observation of the sediment concentration in the inundating tsunami flows, and thus, it is impossible to compare the reconstruction with the actual observation. Goto et al. (2014) estimated the sediment concentration of the 2011 Tohoku-Oki tsunami as roughly 2 vol.% based on the ratio of thickness of tsunami deposits and the inundation depth. This estimate is smaller than the predicted values in this study. However, from the turbid water remained in the box after the tsunami, Arikawa (2019) recently reported that the tsunami flow reached 1,130 kg/m^3 in density that corresponds to approximately 6 vol.%, which is close to the prediction by the inverse models proposed in this study.

The predicted results for the maximum flow depth were also very close to the observed maximum flow depth in the field data (Figure 13). The model predicted 4.11 m that approximates the observed values well. The uncertainty analysis performed using the jackknife method indicated that the error of estimates ranges from 3.8 m to 4.4 m, which is reasonably narrow for an assessment of the magnitude of the tsunami. However, considering the reconstruction bias of the maximum flow depth that was detected when the inverse models were tested using the artificial data, 0.5 m should be added to the maximum flow depth predicted by the inverse models (Figure 11c). Thus, the reconstructed values obtained using the model may be corrected to 4.6 m, which is closer to the observed data set.

5.3 Comparison with existing models

In the present study, we presented the use of a deep-learning NN as an inversion technique with a modified FITTNUSS forward model to obtain the initial tsunami hydraulic condition based on tsunami deposits. The advantages of this new methodology are that (1) it can employ a more realistic forward model than previous methods, and (2) the performance of the inverse model can be tested before its application to actual deposits by using artificial data sets. In addition, (3) it is possible to conduct an uncertainty analysis of the inversion using the resampling method owing to the computational efficiency of the model.

Firstly, the DNN inverse model can employ the forward model, which is computationally expensive. The new inverse model requires only a limited number of iterations of the forward model calculation for producing the training data sets, and these iterations can be parallelized. The calculation for producing each training data set is independent. In contrast, the previous inverse models, including the FITTNUSS model (Naruse & Abe, 2017), employed the optimization method (e.g., L-BFGS) in which the forward model calculation depends on the result of the previous iteration, and thus, this trial and error procedure cannot be parallelized. It was time consuming to obtain the best solution and was difficult to improve the computational efficiency in the previous methodology. Therefore, the previous inverse model only employed the largely abridged forward models such as the "moving-settling tube" (Soulsby et al., 2007) or sudden settling from equilibrium uniform flows (B. E. Jaffe & Gelfenbuam, 2007). The recent inverse model TSUFLIND (Tang et al., 2018; Tang & Weiss, 2015) also probably employed a similar simplified assumption because of this computational load problem. In the new inverse model, this limitation is diminished in the forward model, such that the former can potentially employ fully hydrodynamic models as the forward model.

Secondly, the inverse model proposed herein can be tested prior to the actual analysis because each inversion (i.e., feed-forward calculation of the NN) is completed instantaneously in this method. In previous methods, such as FITTNUSS, each inversion requires a long time such that it was not realistic to iterate the inversion several hundred times for testing the performance of the model. In addition, a modern statistical uncertainty analysis requires resampling procedures in which the iteration of the inversion is also required. Therefore, it was possible to apply the jackknife uncertainty analysis in the case of the DNN inversion in this study, but it is difficult to provide an error range of the estimates for the FITTNUSS method or other methods in a realistic time period.

6 Limitation and scope of improvement

The present model shows promising results, but the reliability of this model is required to be validated by using more field data. The options and hyperparameters of the inversion, such as the sampling window size, can be tested using other examples of modern tsunami deposits with known flow parameters. Furthermore, it is necessary to apply this model to tsunami deposits in Tohoku and other regions along with older tsunami

deposits in order to scrutinize the present model comprehensively and to develop a robust model that can be used in the relevance of hazard evaluation.

In addition, the model still has some limitations in terms of its applicability and accuracy. For example, the reconstructed values of the maximum flow depth showed a bias of -0.5 m, and the cause of this bias is unknown. However, in deciphering other parameters such as the maximum inundation length, flow velocity, and sediment concentration, this model showed satisfactory results for tsunamis of any scale. Currently, this model can only be applied to flat coastal areas and does not incorporate a steeply sloping surface or topographically complicated regions. Nevertheless, these limitations can be overcome by further modifications to the forward model because the DNN inversion model can potentially incorporate complete hydrodynamic models as the forward model.

7 Conclusion

The new model presented in this study uses an artificial NN to derive the hydraulic conditions of a tsunami. It successfully reconstructed the flow conditions including the maximum inundation length, flow velocity, maximum flow depth and sediment concentrations from artificial tsunami deposits produced by the forward model as well as the natural tsunami deposits of 2011 Tohoku-Oki tsunami. The reconstructed flow velocity and maximum depth were 5.4 m/sec and 4.11 m respectively, which are in the ranges of observed values of the tsunami. The uncertainty of the results was determined using the jackknife method, which also shows that the model yields results that do not comprise large ranges of data. Thus, in future studies, it is expected that this model would be able to successfully reconstruct the flow conditions of modern and ancient tsunamis.

Acknowledgments

The source codes and all other data of DNN inverse model are available in Zenodo (`https://doi.org/10.5281/zenodo.3685480`), which is the open access data repository. We express our sincere gratitude to Prof. Takao Ubukata and other researchers in the biosphere study group of Kyoto University for their valuable suggestions. We thank Sediment Dynamics Research Consortium (sponsored by INPEX, JOGMEC, JX Nippon Oil & Gas Exploration Corporation) for funding. The authors thank Kyoto University for providing access to the required facilities and the Ministry of Education, Cul-

ture, Sports, Science and Technology, Japan, for providing the permission and scholarship for conducting this collaborative research in Japan.

References

Abdi, H., & Williams, L. J. (2010). Jackknife. *Encyclopedia of research design*, *2*.

Abe, T., Goto, K., & Sugawara, D. (2012). Relationship between the maximum extent of tsunami sand and the inundation limit of the 2011 tohoku-oki tsunami on the sendai plain, japan. *Sedimentary Geology*, *282*, 142–150.

Arikawa, T. (2019). *The threat of the "black tsunami" revealed.* `https://www.nhk.or.jp/special/plus/articles/20190314/index.html`. (Accessed: 2019-04-12)

Bishop, C. M., et al. (1995). *Neural networks for pattern recognition*. Oxford university press.

Bourke, P. (1999). Interpolation methods. *Miscellaneous: projection, modelling, rendering.*(1).

Choowong, M., Murakoshi, N., Hisada, K.-i., Charusiri, P., Charoentitirat, T., Chutakositkanon, V., ... Phantuwongraj, S. (2008). 2004 indian ocean tsunami inflow and outflow at phuket, thailand. *Marine Geology*, *248*(3-4), 179–192.

Costa, P. J., Andrade, C., Cascalho, J., Dawson, A. G., Freitas, M. C., Paris, R., & Dawson, S. (2015). Onshore tsunami sediment transport mechanisms inferred from heavy mineral assemblages. *The Holocene*, *25*(5), 795–809.

Crank, J. (1984). *Free and moving boundary problems*. Clarendon press Oxford.

Dietrich, W. E. (1982). Settling velocity of natural particles. *Water resources research*, *18*(6), 1615–1626.

Farrell, P. J., & Singh, S. (2010). Some contributions to jackknifing two-phase sampling estimators. *Survey Methodology*, *36*(1), 57–68.

Foytong, P., Ruangrassamee, A., Shoji, G., Hiraki, Y., & Ezura, Y. (2013). Analysis of tsunami flow velocities during the march 2011 tohoku, japan, tsunami. *Earthquake Spectra*, *29*(s1), 161–181.

Ganti, V., Chu, Z., Lamb, M. P., Nittrouer, J. A., & Parker, G. (2014). Testing morphodynamic controls on the location and frequency of river avulsions on fans versus deltas: Huanghe (yellow river), china. *Geophysical Research Letters*,

41(22), 7882–7890.

Ghobarah, A., Saatcioglu, M., & Nistor, I. (2006). The impact of the 26 december 2004 earthquake and tsunami on structures and infrastructure. *Engineering structures*, *28*(2), 312–326.

Goto, K., Hashimoto, K., Sugawara, D., Yanagisawa, H., & Abe, T. (2014). Spatial thickness variability of the 2011 Tohoku-oki tsunami deposits along the coastline of Sendai Bay. *Marine Geology*, *358*, 38–48.

Hayashi, S., & Koshimura, S. (2013). The 2011 tohoku tsunami flow velocity estimation by the aerial video analysis and numerical modeling. *Journal of Disaster Research*, *8*(4), 561–572.

Hirano, M. (1971). River bed degradation with armoring. *Proceedings of Japan Society of Civil Engineers*, *1971*(195), 55–65.

Ian, G., & Yoshua, B. (2016). *Deep learning (adaptive computation and machine learning)*. MIT Press, Cambridge.

Imamura, F., Boret, S. P., Suppasri, A., & Muhari, A. (2019). Recent occurrences of serious tsunami damage and the future challenges of tsunami disaster risk reduction. *Progress in Disaster Science*, *1*, 100009.

Jaffe, B., Goto, K., Sugawara, D., Gelfenbaum, G., & La Selle, S. (2016). Uncertainty in tsunami sediment transport modeling. *Journal of Disaster Research*, *11*(4), 647–661.

Jaffe, B. E., & Gelfenbuam, G. (2007). A simple model for calculating tsunami flow speed from tsunami deposits. *Sedimentary Geology*, *200*(3-4), 347–361.

Jaffe, B. E., Goto, K., Sugawara, D., Richmond, B. M., Fujino, S., & Nishimura, Y. (2012). Flow speed estimated by inverse modeling of sandy tsunami deposits: results from the 11 march 2011 tsunami on the coastal plain near the sendai airport, honshu, japan. *Sedimentary Geology*, *282*, 90–109.

Jerolmack, D. J., & Paola, C. (2010). Shredding of environmental signals by sediment transport. *Geophysical Research Letters*, *37*(19).

Johnson, J. P., Delbecq, K., & Kim, W. (2017). Predicting paleohydraulics from storm surge and tsunami deposits: Using experiments to improve inverse model accuracy. *Journal of Geophysical Research: Earth Surface*, *122*(4), 760–781.

Jordan, M. I., & Rumelhart, D. E. (1992). Forward models: Supervised learning

with a distal teacher. *Cognitive science*, *16*(3), 307–354.

Lin, A., Ikuta, R., & Rao, G. (2012). Tsunami run-up associated with co-seismic thrust slip produced by the 2011 mw 9.0 off pacific coast of tohoku earthquake, japan. *Earth and Planetary Science Letters*, *337*, 121–132.

Madsen, O., Wright, L., Boon, J., & Chisholm, T. (1993). Wind stress, bed roughness and sediment suspension on the inner shelf during an extreme storm event. *Continental Shelf Research*, *13*(11), 1303–1324.

Moore, G., Bangs, N., Taira, A., Kuramoto, S., Pangborn, E., & Tobin, H. (2007). Three-dimensional splay fault geometry and implications for tsunami generation. *Science*, *318*(5853), 1128–1131.

Mori, N., Takahashi, T., & Group, . T. E. T. J. S. (2012). Nationwide post event survey and analysis of the 2011 tohoku earthquake tsunami. *Coastal Engineering Journal*, *54*(1), 1250001–1.

Nakajima, H., & Koarai, M. (2011). Assessment of tsunami flood situation from the great east japan earthquake. *Bull Geospatial Info Authority Japan*, *59*, 55–66.

Naruse, H., & Abe, T. (2017). Inverse tsunami flow modeling including nonequilibrium sediment transport, with application to deposits from the 2011 tohoku-oki tsunami. *Journal of Geophysical Research: Earth Surface*, *122*(11), 2159–2182.

Nisbet, R., Elder, J., & Miner, G. (2009). *Handbook of statistical analysis and data mining applications*. Academic Press.

Patterson, J., & Gibson, A. (2017). *Deep learning: A practitioner's approach*. " O'Reilly Media, Inc.".

Quenouille, M. (1949, 01). Approximate tests of correlation in time-series. *Journal of the Royal Statistical Society B*, *11*, 68-84.

Rijn, L. C. v. (1984). Sediment transport, part ii: suspended load transport. *Journal of hydraulic engineering*, *110*(11), 1613–1641.

Romano, M., Liong, S.-Y., Vu, M. T., Zemskyy, P., Doan, C. D., Dao, M. H., & Tkalich, P. (2009). Artificial neural network for tsunami forecasting. *Journal of Asian Earth Sciences*, *36*(1), 29–37.

Saatcioglu, M., Ghobarah, A., & Nistor, I. (2005). Effects of the december 26, 2004 sumatra earthquake and tsunami on physical infrastructure. *ISET J. Earthq. Technol*, *42*, 79–94.

Shephard, F., Macdonald, G., & Cox, D. (1950). The tsunami of april, 1946. *Scripps Inst. Oceanog. Bull*, *5*(6), 391–528.

Smith, D., Foster, I., Long, D., & Shi, S. (2007). Reconstructing the pattern and depth of flow onshore in a palaeotsunami from associated deposits. *Sedimentary Geology*, *200*(3), 362–371.

Smith, J., & Eli, R. N. (1995). Neural-network models of rainfall-runoff process. *Journal of water resources planning and management*, *121*(6), 499–508.

Smith, S. (2013). *Digital signal processing: a practical guide for engineers and scientists*. Elsevier.

Soulsby, R. L., Smith, D. E., & Ruffman, A. (2007). Reconstructing tsunami run-up from sedimentary characteristics—a simple mathematical model. In *Coastal sediments* (Vol. 7, pp. 1075–1088).

Srivastava, N., Hinton, G., Krizhevsky, A., Sutskever, I., & Salakhutdinov, R. (2014). Dropout: a simple way to prevent neural networks from overfitting. *The journal of machine learning research*, *15*(1), 1929–1958.

Sugawara, D., Goto, K., & Jaffe, B. E. (2014). Numerical models of tsunami sediment transport—current understanding and future directions. *Marine Geology*, *352*, 295–320.

Sutskever, I., Martens, J., Dahl, G., & Hinton, G. (2013). On the importance of initialization and momentum in deep learning. In *International conference on machine learning* (pp. 1139–1147).

Tang, H., Wang, J., Weiss, R., & Xiao, H. (2018). Tsuflind-enkf: Inversion of tsunami flow depth and flow speed from deposits with quantified uncertainties. *Marine Geology*, *396*, 16–25.

Tang, H., & Weiss, R. (2015). A model for tsunami flow inversion from deposits (tsuflind). *Marine geology*, *370*, 55–62.

Yoshikawa, Y., & Watanabe, Y. (2008). Examine of Manning's coefficient and the bed-load layer for one-dimensional calculation of bed variation. *Monthly Report of Civil Engineering Research Institute for Cold Region*, *662*, 11–20.